Modelling, Simulation, and Optimisation Experiment: Wheat Threshing Process of Combine Harvester Based on DEM

Q. Li^{1, 2*}, Y. Wu¹, K. Zhao¹, H. Wang², J. Ji^{1, 2}

- 1- College of Agricultural Equipment Engineering, Henan University of Science and Technology, Luoyang 471003, China
- 2- Science & Technology Innovation Center for Completed Set Equipment, Longmen Laboratory, Luoyang 471023, China
- (*- Corresponding Author Email: liqw0613@163.com) https://doi.org/10.22067/jam.2025.94433.1409

Abstract

Grain loss and impact damage are key indicators of wheat threshing quality. To explore the mechanisms of grain loss and damage, this study reproduces the wheat threshing process by establishing a discrete element model of wheat plants and a simulation platform for threshing devices. It conducts simulations on the movement laws of material flow and distribution laws of threshed materials under different conditions of feed rate, drum rotational speed, and deflector angle. Based on simulation calculations, the average velocity and force laws of wheat plants were obtained, and the influence laws of feed rate, drum rotational speed, and deflector angle on the threshing process were analysed. Through multi-objective parameter optimisation analysis, it is determined that when the feed rate is 7 kg s⁻¹, the drum rotational speed is 815 r min⁻¹, and the deflector angle is 70 degrees, the threshing performance of the device is relatively superior. Bench verification tests before and after optimisation showed that the impurity rate of wheat decreased from 29.19% to 25.02%, and the loss rate decreased from 1.61% to 0.95%, with the error between the model prediction results and the experimental results being less than 5%. The proposed model and optimisation strategy can directly guide the structural improvement of axial-flow threshing devices, significantly shorten the research and development cycle of harvesting equipment, and provide a reliable technical basis for efficient and low-loss wheat harvesting.

Keywords: Discrete element method, Parameter optimisation, Simulation analysis, Threshing device, Work performance

Introduction

The threshing device is the core component of the combine harvester, and its working performance has become the main factor restricting the development of the combine harvester. During the harvesting process, grain loss and damage are significantly affected by the performance of the threshing devices (Fu, Chen, Han, & Ren, 2018; Khir, Atungulu, & Pan, 2013; Zareiforoush, Komarizadeh, & Alizadeh, 2010). Therefore, many researchers are dedicated to studying grain threshing devices.

Traditional performance test methods for threshing devices are usually bench or field tests, which infer their functions, characteristics, and operating laws by observing the relationship between input and output. This test method has the problems of high cost, poor repeatability, long cycle, and high labour demand, resulting in a series of excessively lengthy and complex procedures.

The Discrete Element Method, as a new type of numerical analysis method, has begun to be applied in various links such as planting, harvesting, threshing, cleaning, transportation in the process of agricultural operations (Ajmal, Roessler, Richter, Katterfeld, 2020; Boac, Ambrose, Casada, Maghirang, & Maier, 2014; Horabik Molenda, 2016). Miu and Kutzbach (2008b) established a simulation model of the axialthreshing device, reproducing threshing and separation processes of wheat. Shi et al. (2019) obtained the optimal combination of operating parameters affecting the working performance of the straw crushing drill-type conservation tillage seeder through simulation and numerical analysis methods,

and the straw coverage uniformity of the optimised seeder reached 86.25%. W. Wang et al. (2020) adopted the EDEM-Recurdyn coupling method to analyse the migration laws, velocity, and flow rate changes of wheat during the continuous conveying process, and the results showed that the error between the experiment and simulation was 4.08%. Siliveru and Ambrose (2021) used the Discrete Element Method to partially reconstruct the wheat milling process, predicted the sieving behaviour of flour particles, and the range of predicted standard errors was 0.13-8.27%. Markauskas, Platzk, and Kruggel-Emden (2022) explored the pneumatic conveying mechanism of wheat straw in elbow conveying using the Discrete Element Method, and the results showed that the trajectory and pressure drop of particles in vertical pipe sections depend on the stiffness of the particles. Sun et al. (2023) adopted the Discrete Element Method to construct a wheat plant model, and conducted vibration screening tests and impact threshing tests to verify the accuracy of the model. These studies have laid a foundation for analysing the wheat harvesting process using the Discrete Element Method.

In summary, the effectiveness of the discrete element method (DEM) simulation technology in wheat production processes has been confirmed. However, most DEM simulation frameworks for wheat threshing processes rely on modelling-simulation, simulation-optimisation, or simulation-validation, and rarely form a closed-loop of "modelling-calibration-simulation-

optimisation-validation." On the other hand, due to the enclosed nature of the threshing process, research on grain loss and impact damage is limited. This study has conducted preliminary research on the mechanisms of grain loss and impact damage indirectly by verifying the effectiveness of the simulation through grain distribution.

Accordingly, to explore the mechanisms of grain loss and impact damage of wheat in the threshing device, as well as the interaction mechanism between wheat and the threshing device, this study reproduces the wheat

threshing process by establishing a discrete element model of wheat plants and a simulation platform for the threshing device. Combined with the test bench, the working performance of the threshing device was verified. The feed rate, drum rotational speed, and guide plate angle were analysed for their effects on the kinematic and dynamic responses of wheat within the threshing device. This study aims to reveal the variation trend of the interaction mechanism between wheat and the threshing device under different levels of influencing factors, as well as the influence law of such interaction mechanism on the operating performance of the threshing device under varying factor levels. The main contributions of this work are as follows: (1) With respect to the construction methodology of discrete element method (DEM) simulation models for wheat threshing processes, an integrated workflow incorporating modelling, simulation, and validation was established. This framework provides a viable technical route for the application of DEM simulation technology in the threshing process of combine harvesters. (2) Velocities and force laws of wheat during threshing, obtained via simulation, reveal the coupled effects of parameters such as feed rate, drum speed, and deflector angle on grain loss and impurity rates. This provides quantitative support for improvement performance the and enhancement of threshing devices, and such laws are difficult to acquire through traditional experiments. (3) DEM simulation predicts the operational performance of wheat threshing devices under varying parameters, with model accuracy validated via bench and field tests. This demonstrates that combining DEM with response surface methodology analysing device performance, predicting threshing outcomes, and enhancing research development efficiency of harvesting equipment.

Materials and Methods

Discrete Element Model of wheat plants

Calibrating the physical properties and contact characteristic parameters of wheat is a

prerequisite for the reasonable prediction of wheat behaviour. This study measured and statistically analysed 600 wheat plants, explored the distribution characteristics of different structures of wheat, and provided theoretical support for establishing a model. The constructed model of wheat is shown in Fig. 1. The test materials were sampled in

Zhengzhou City, Henan Province, China, from June 1 to 3, 2024, with the variety being "Xumai 35". Materials for the bench tests were manually harvested and brought back to the laboratory for measurement; the basic parameters of wheat obtained from the measurements are shown in Table 1.

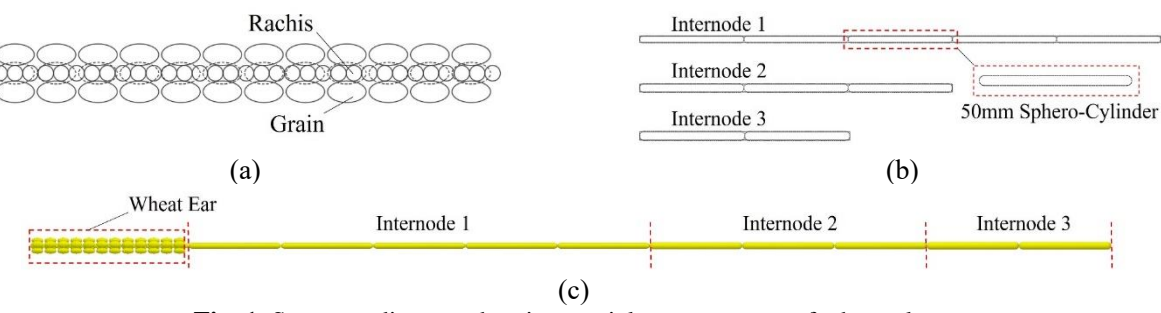


Fig. 1. Structure diagram showing particle arrangement of wheat plant: (a) Rachis, (b) Internode of the stem, and (c) Wheat plant

Table 1- Basic properties of test materials

Parameter	Values
Plant height after stubble cutting	477-734 mm
Length of ear	76.7-99.7 mm
Ratio of straw to grain	1: 1.2
Thousand grain weight	40.87-42.72 g
Grain moisture content	13.42-17.54%
Straw moisture content	18.04-25.47%

The model parameters of each component of wheat plants were determined via direct measurement, slope test, tensile test, compression test, shear test, bulk density test, angle of repose test, and other methods. In Fig. 2, the measurement process is presented. Firstly, the physical property parameters of wheat plants were directly measured using equipment such as electronic balances, density bottles, and vernier callipers. Subsequently, the contact characteristic parameters of wheat

plants were determined through slope tests, bulk density tests, and angle of repose tests, and the parameter results were optimised. Finally, the mechanical property parameters of wheat plants were determined through tensile tests, compression tests, and shear tests. The remaining parameters were determined from the references. The parameters in the simulation are presented in Table 2 and Table 3.

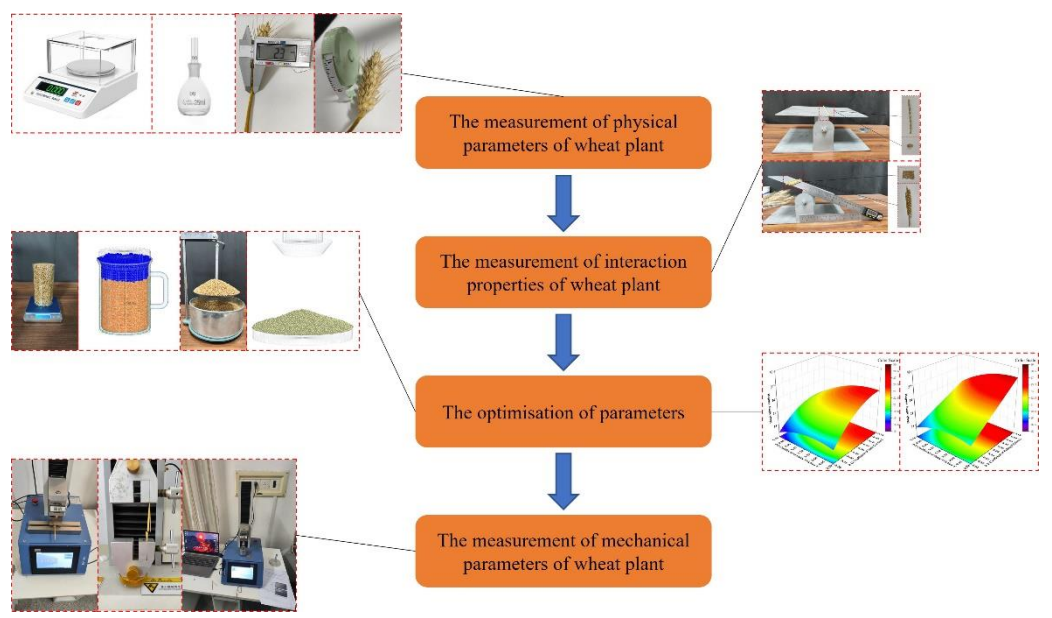


Fig. 2. The measurement process of wheat plant parameters

Table 2- Main parameters of wheat plants for the DEM Model

Payameters of wheat plants for the DEM Model Value Value Source				
Parameter	Value	Source Grain		
T	C 1 C			
Length	6.46 mm	Measurement by vernier callipers		
Width	3.62 mm	Measurement by vernier callipers		
Height	3.11 mm	Measurement by vernier callipers		
Number on a wheat ear	46	Measurement through counting		
Density (kg m ⁻³)	1377-1513	Measurement by density bottle		
Poisson's ratio	0.16~0.42	(Arnold & Roberts, 1969; Moya, Sanchez, & Ramon Villar-Garcia, 2022; Standards, 2006)		
Young's modulus (Pa)	$1.35-2 \times 10^{8}$	(Sun et al., 2023)		
	Stem (first	internode/second internode/third internode)		
Length	267/160/110 mm	Measurement by ruler and tape measure		
-	3.58/3.85/4.09	•		
Diameter	mm	Measurement by vernier callipers		
Density (g m ⁻¹)	0.82-2.13	Measurement by ruler and scale		
Poisson's ratio	0.25-0.30	(Khawaja & Khan, 2022; Schramm, Tekeste, Plouffe, & Harby, 2019)		
Young's modulus (Pa)	$1.5 - 6.8 \times 10^9$	Tensile test		
()		Restitution coefficient		
Grain-grain	0.326	Optimisation results		
Grain-steel	0.5-0.75	(Chen, Wassgren, Veikle, & Ambrose, 2020; Horabik, Parafiniuk, & Molenda,		
Character	0.16.0.22	2016; Horabik <i>et al.</i> , 2020; Lu <i>et al.</i> , 2023)		
Straw-straw	0.16-0.32	(Schramm et al., 2019; Shi, Jiang, Wang, Thuy, & Yu, 2023; Sun et al., 2023)		
Straw-steel	0.491-0.593	(Schramm et al., 2019; Sun et al., 2023)		
	0. #00	Static friction coefficient		
Grain-grain	0.588	Slope test and optimisation results		
Grain-steel	0.580	Slope test and optimisation results		
Straw-straw	0.609-0.729	Slope test		
Straw-steel	0.493-0.578	Slope test		
		Rolling friction coefficient		
Grain-grain	0.079	Optimisation results		
Grain-steel	0.023-0.170	Slope test		
Straw-straw	0.012-0.028	(Sun et al., 2023)		
Straw-steel	0.045-0.113	Slope test		

Parameter	Normal stiffness per unit area (N m ⁻³)	Shear stiffness per unit area (N m ⁻³)	Normal stress (MPa)	Shear stress (MPa)
Grain-rachis	1e09	5e08	2e06	2e06
Rachis-rachis	1e09	5e08	1e07	5e06
Straw-rachis	5e09	1e09	1.5e07	4e06
Straw-straw	5e09	1e09	1.5e07	4e06

Longitudinal axial flow threshing test bench and simulation model

The test bench and simulation model of the longitudinal axial flow threshing device used in this study are shown in Fig. 3. The detailed physical characteristics and dimensional parameters of the threshing devices used in the bench tests and simulation models are shown in Table 4. The key components of the threshing device include the screw feeding head, threshing cylinder, concave, and top cover. Prior to the test, wheat plants of a certain mass were evenly spread on one side of the conveyor belt, with a 3-metre acceleration zone reserved. The conveying speed of the conveyor belt was controlled by adjusting the motor speed, thereby regulating the feeding rate of the test. At the start of the test, the threshing device was first adjusted; after it operated stably, the conveyor belt switch was

turned on to feed the materials. The threshed materials. without passing through cleaning system, directly fell into the material receiving boxes below the concave and at the tail of the cylinder. During simulation, wheat plant particles were directly generated by the particle factory above the conveyor belt, and threshing simulation tests were conducted according to the initially set feeding rate. In EDEM, 7-9 kg of wheat plants were generated per second as required by the study, with each wheat plant consisting of 46 particles. The continuous generation time of plants was set to 5 s, and the simulation duration was set to 10 s. The calculation used 10% of the Rayleigh time, with a time step of 4×10^{-7} seconds. Data were saved every 0.01 seconds, and the number of solvers was set to 24.



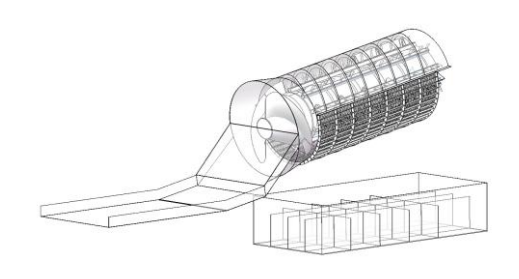


Fig. 3. Wheat threshing device with longitudinal axial flow: (a) Experimental and (b) Simulation platforms

Table 4- Main structural and working parameters of threshing device

Parameter	Value
Diameter of roller	710 mm
Length of roller	1850 mm
Adjustable range of rotational speed of roller	0-1150 rpm
Adjustable range of angle of deflector	60-80 degrees

Field trials validation

To verify the accuracy of the predictions from the simulation and parameter optimisation model, a verification test was conducted on June 1, 2025, in the experimental field of Yiyang County, Luoyang City, China. The operating parameters adopted were the optimal parameter combination

derived from the model: a feeding rate of 7 kg s⁻¹, a drum rotational speed of 815 r min⁻¹, and a deflector angle of 70 degrees. During the test, key operating scenarios and loss observation points were recorded (Fig. 4): (a) Overall view of the field test site, showing the operating status of the harvester in the wheat field; (b) Threshing drum, where grain losses remaining in the drum were measured; (c)

Cleaning sieve, where grain losses remaining on the sieve plate were measured; (d) Field ground, where entrainment and unthreshed losses were evaluated by collecting and analysing scattered grains. The test data collected from these observations were further used to verify the reliability of the model's prediction results.



Fig. 4. Field trial: (a) Test site, (b) Drum losses, (c) Clearance losses, and (d) Entrainment and uncleaned losses

Results

Threshing Simulation Validation

After threshing, the materials in the material receiving boxes at the bottom of the threshing device were collected and counted, and the percentage of grain mass in each small box relative to the total grain mass was calculated. Based on the grid numbers, the grain mass distribution curve in the material receiving box was plotted, as shown in Fig. 5. The absolute error of grain mass in each material receiving box ranges from 0.09% to 4.43%, and the simulation well reproduces the results of the bench test. To enhance the

persuasiveness of this explanation, this study employs Spearman's rank correlation coefficient to conduct further data analysis on the correlation between the two curves. For the original data X_i and Y_i , the correlation coefficient r_s can be expressed as:

$$r_s = \frac{\text{cov}(R(X), R(Y))}{\sigma_{R(X)}\sigma_{R(Y)}}$$
(1)

where, cov(R(X), R(Y)) is the covariance of variables, and $\sigma_{R(X)}\sigma_{R(Y)}$ is the standard deviation of variables.

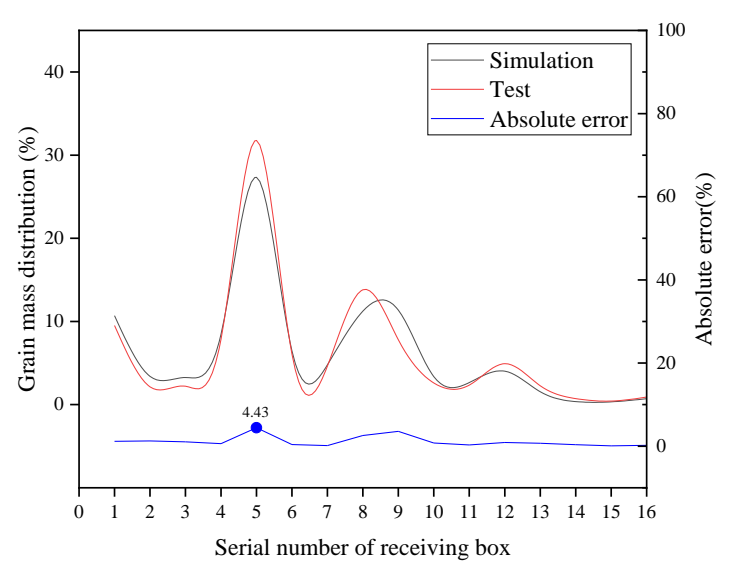
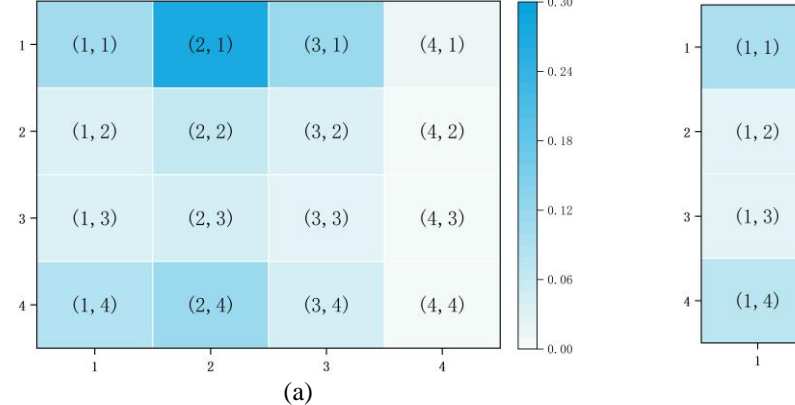


Fig. 5. Trend in grain mass distribution variation

The results show that the Spearman's rank correlation coefficient is 0.94, indicating that the test results and simulation results have a positive correlation and share the same changing trend.

To more intuitively observe the law of grain distribution, this study respectively plotted heatmaps of the simulation results and bench test results regarding the grain mass distribution at the bottom of the wheat plants' threshing device, as shown in Fig. 6. The two heatmaps use the same colour scale for representation. According to the analysis of the heatmaps, grains are mainly distributed

between (1, 1) and (2, 4), with a higher distribution at (1, 1), (1, 4), (2, 1), and (2, 4). Generally, it shows a trend where there are more grains on both sides of the rows and fewer in the middle, and more grains in the front of the columns and fewer in the rear. This is because, as the cylinder rotates, wheat grains are subjected to the tangential impact force of the cylinder. Due to inertia, wheat grains tend to move in the tangential direction and finally fall into the outer material receiving boxes after hitting the cylinder walls on both sides.



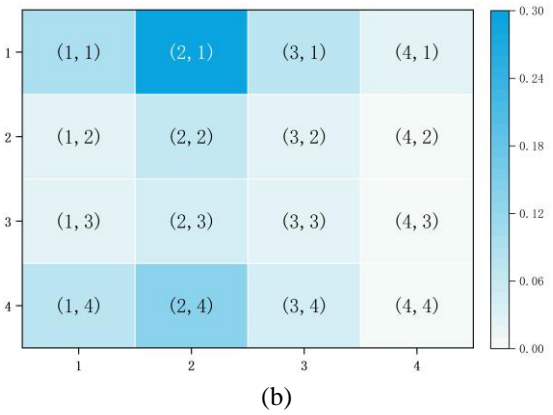


Fig. 6. Grain mass distribution change trend heatmap: (a) Simulation and (b) Test

Analysis of the Movement Law of Wheat Plants

The movement speed and the magnitude of impact force of wheat plants in the threshing

device were exported through the postprocessing function of EDEM, so as to further analyse the movement law of wheat plants in the threshing device. Here, wheat plants are considered to consist of two parts: grains and stems. The threshing device is equidistantly divided into four sections from the feeding end to the tail of the cylinder, namely the feeding section, threshing section, separating section, and impurity discharging section. During the

simulation, the feeding rate was 4 kg s⁻¹, the conveyor belt speed was 2 m s⁻¹, the drum rotational speed was 800 rpm, and the guide plate angle was 70 degrees. The exported data are shown in Fig. 7, where the velocity and impact force of wheat plants within the range of 0~8s are recorded for each section.

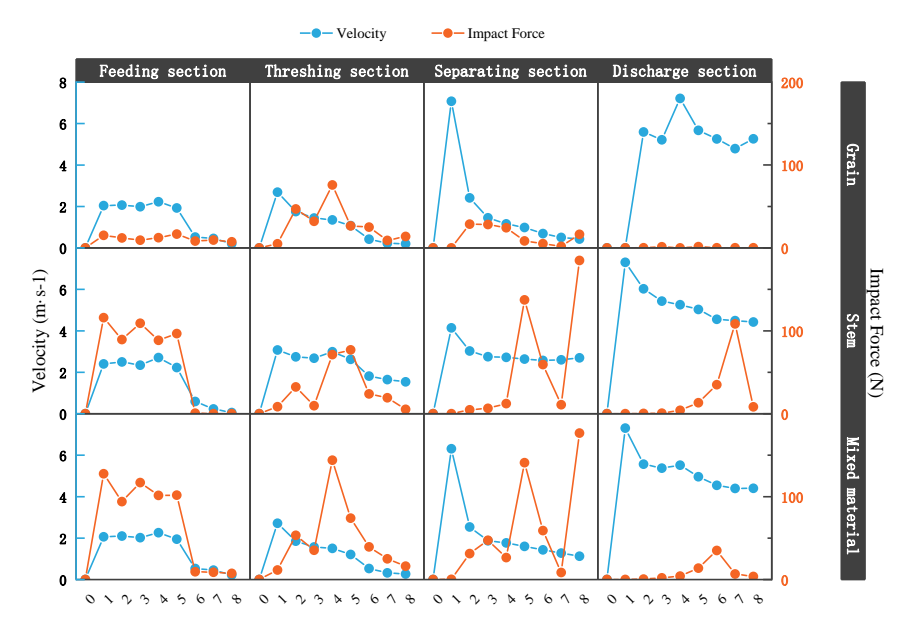


Fig. 7. Average impact force and velocity for wheat plants

Within the feeding section, the initial velocity of grains is close to the conveyor belt speed (2 m s⁻¹), and the impact force they are subjected to is usually less than 5 N, which is far lower than the force required for threshing. The stem velocity gradually accelerates from an initial low speed to a velocity matching the inlet of the threshing section $(0~3 \text{ m s}^{-1})$, slightly higher than the grain velocity), and the impact force it undergoes shows a slight increase. This indicates that the core function of the feeding section is to uniformly and continuously feed the plants into the threshing section through the feeding head, focusing on avoiding blockage rather than threshing. At this point, grains are still attached to the ears (not separated from the stems) and move along with the overall movement of the stems. As the carrier of grains, stems dominate the movement of grains during the feeding process and move axially under the spiral propulsion of the feeding head and guide plate.

Within the threshing section, the grain velocity decreases from slightly greater than the conveyor speed to 0, exhibiting a significant difference from the stem velocity. This indicates that the movement of grains is no longer dominated by the stems. The impact forces on grains and stems underwent a process of drastic change: the impact force from the drum on grains and stems surged to 76 N, which serves as the direct driving force for grain detachment.

Within the separating section, grains exhibit the same movement characteristics as those in the threshing section. The sudden increase in velocity at 1 s is related to the impacts from the feeding section and threshing section; the struck grains and stems, with higher velocities, reach the separating section first. Unlike the threshing section, during this stage, stems are subjected to intense and unstable impact forces, which are jointly generated by the impact of drum teeth and the extrusion of the

concave plate, resulting in stem breakage.

Within the impurity discharging section, the magnitude of grain velocity is consistent with that of stem velocity, while the impact force they are subjected to is almost zero. This indicates that within this section, the grain velocity is dominated by the stems, and there exist unthreshed grains that are discharged along with the stems. The materials are mainly transported by the pushing force and frictional force of the impurity discharging components, which only maintain their movement toward the impurity discharge port without a significant threshing effect.

Response Surface Experiment and Analysis

To improve the working performance of the wheat axial-flow threshing device, a three-factor and three-level response surface experiment was simulated using EDEM, with feeding rate, drum rotational speed, and guide plate angle as the experimental factors. Response surface optimisation design is a statistical analysis method that finds the

optimal parameter combination through experimental design and mathematical modelling, and it is a commonly used method in discrete element method and parameter optimisation of agricultural machinery (Luo et al., 2023; Shi et al., 2023; Wang, Wu, & Jia, 2023; Zhou et al., 2023). The factors and level coding of the response surface experiment for wheat threshing model parameters are shown in Table 5. The design scheme and results of the response surface optimisation experiment are presented in Table 6, where all nonexperimental factors were set to level 0.

Design-Expert was used to perform fitting analysis on the design scheme and experimental results in Table 6, and a ternary quadratic polynomial regression model of wheat impurity rate Y_1 with respect to feeding rate X_1 , drum rotational speed X_2 , and guide plate angle X_3 was established as shown in Equation (2). The significance test table of the regression equation is presented in Table 7.

$$Y_1 = 27.24 + 1.75X_1 + 2.49X_2 + 2.04X_3 + 0.523X_2X_3 + 1.37X_2^2 + 1.05X_3^2$$
 (2)

Table 5- Coding of factors

Factor	Low level	0 level	High level
Feeding rate	7	8	9
Rotational speed of roller	700	800	900
Angle of deflector	65	70	75

Table 6- Experimental design and results of threshing test for wheat

No.	Feeding rate X ₁	Rotational speed of roller X2	Angle of deflector X ₃	Impurity rate Y ₁	Loss rate Y ₂
1	-1	-1	0	24.44	1.26
2	-1	0	-1	24.17	1.27
3	1	0	-1	28.03	1.38
4	0	-1	1	28.47	1.24
5	0	1	1	34.92	1.04
6	0	1	-1	29.85	1.26
7	0	-1	-1	25.73	1.60
8	1	0	1	31.96	1.08
9	1	1	0	32.58	1.08
10	0	0	0	27.38	1.01
11	0	0	0	27.47	1.04
12	-1	0	1	28.72	1.01
13	1	-1	0	27.96	1.32
14	0	0	0	27.19	1.02
15	-1	1	0	29.16	0.92

Table 7- Regression equation variance analysis of impurity rate					
Sources	Sum of squares	Degree of freedom	Mean Square	F values	P values
Model	119.08	6	19.85	323.39	< 0.0001
X_1	24.64	1	24.64	401.49	< 0.0001
X_2	49.55	1	49.55	807.4	< 0.0001
X_3	33.17	1	33.17	540.49	< 0.0001
X_2X_3	1.36	1	1.36	22.12	0.0015
X_2^2	6.95	1	6.95	113.31	< 0.0001
X_3^2	4.12	1	4.12	67.14	< 0.0001
Residual	0.491	8	0.0614		
Lack of fit	0.4501	6	0.075	3.67	0.2295
Pure error	0.0409	2	0.0204		
Total sum	119.57	14			

Note: P < 0.01 (highly significant); $0.01 \le P < 0.05$ (significant); $P \ge 0.1$ (not significant). The same as below.

A ternary quadratic polynomial regression model of wheat loss rate Y_2 with respect to feeding rate X_1 , drum rotational speed X_2 , and guide plate angle X_3 was established, as shown in Equation (3), and the significance test table

of the regression equation is presented in Table 8.

$$Y_2 = 1.03 + 0.05X_1 - 0.14X_2 - 1.43X_3 + 0.03X_1X_2 + 0.04X_2X_3 + 0.11X_2^2 + 0.15X_3^2$$
(3)

Table 8- Regression equation variance analysis of loss rate

Sources	Sum of squares	Degree of freedom	Mean Square	F values	P values
Model	0.467	7	0.0667	266.87	< 0.0001
X_1	0.02	1	0.02	80	< 0.0001
X_2	0.1568	1	0.1568	627.2	< 0.0001
X_3	0.1624	1	0.1624	649.8	< 0.0001
X_1X_2	0.0025	1	0.0025	10	0.0159
X_2X_3	0.0049	1	0.0049	19.6	0.0031
X_{2}^{2}	0.0449	1	0.0449	179.77	< 0.0001
X_3^2	0.0836	1	0.0836	334.29	< 0.0001
Residual	0.0018	7	0.0003		
Lack of fit	0.0013	5	0.0003	1.1	0.5395
Pure error	0.0005	2	0.0002		
Total sum	0.4688	14			

It can be seen from Table 7 and Table 8 that the P-value of the model is less than 0.01, and the P-value of the lack of fit term is greater than or equal to 0.1, indicating that the regression model can be used for experimental analysis. Both the impurity rate Y_1 and the loss rate Y_2 exhibit a quadratic function relationship with the drum rotational speed X_2 and the guide plate angle X_3 , and a linear function relationship with the feeding rate X_1 .

From the results of the F-value test, the drum rotational speed has the largest range of influence on the impurity rate of threshed materials, while the feeding rate has the smallest range of influence. The reason for this is that an increase in drum rotational speed

intensifies stem breakage, and broken stems are more likely to be discharged through the concave plate. The guide plate angle affects the movement speed of the material flow in the threshing chamber. Generally, the larger the axial angle of the guide plate, the slower the movement speed of the material flow, the longer the residence time of stems, and the more times they are struck. The feeding rate affects the thickness of the material layer. As the feeding rate increases, the spatial density in the threshing chamber relatively increases, and the gap between the material layer and the threshing chamber relatively decreases, leading to an increase in the degree of material fragmentation and a consequent increase in the

impurity rate of threshed materials.

By contrast, the guide plate angle exerts the most significant influence on the loss rate of threshed materials. As the drum rotational speed and guide plate angle increase, the loss rate exhibits a trend of first decreasing and then increasing. This is because a smaller guide plate angle increases the flow resistance of materials, leading to material accumulation, with some materials being directly discharged in a compressed state. A larger guide plate angle accelerates the flow velocity of materials, resulting in insufficient effective interaction between plants and threshing elements, which causes some grains to fail to separate from the rachis. At lower drum rotational speeds, the impact force of threshing elements on plants is insufficient, and the total loss rate is dominated by unthreshed loss; the loss rate increases because materials are not sufficiently threshed. At higher rotational speeds, excessive centrifugal force may directly throw incompletely threshed ears out of the threshing chamber. Meanwhile, stem breakage increases, and a large number of grains are discharged along with broken stems, leading to a sharp increase in entrainment loss. The loss rate increases with the increase in the

feeding rate. This is because excessively high material density forms a protective layer that prevents internal grains from being threshed; meanwhile, it blocks internal grains from separating out of the threshing chamber, resulting in an increase in entrainment loss and unthreshed loss.

By setting $X_1 = X_2 = 0$, $X_1 = X_3 = 0$, and $X_2 = 0$ $X_3=0$, respectively, the patterns of influence of interaction factors X_1X_2 , X_1X_3 , and X_2X_3 on the impurity rate Y_1 and loss rate Y_2 were obtained, as shown in Fig. 8. It can be seen from Fig. 8a that the drum rotational speed X₂ has a relatively significant influence on the interaction with the impurity rate Y₁, and the impurity rate of threshed materials is the minimum when $X_2 = -1$ and $X_3 = -1$. It can be seen from Fig. 8b that in the interaction between the feeding rate X_1 and the drum rotational speed X_2 on the loss rate Y_2 , the drum rotational speed has a more significant influence on the interaction, and the loss rate reaches the maximum when $X_1 = -1$ and $X_2 = 1$. It can be seen from Fig. 8c that the drum rotational speed and the guide plate angle exert a roughly similar influence on the loss rate. The loss rate is minimised when $X_2=0$ and $X_3=0$, as well as when $X_2=1$ and $X_3=1$.

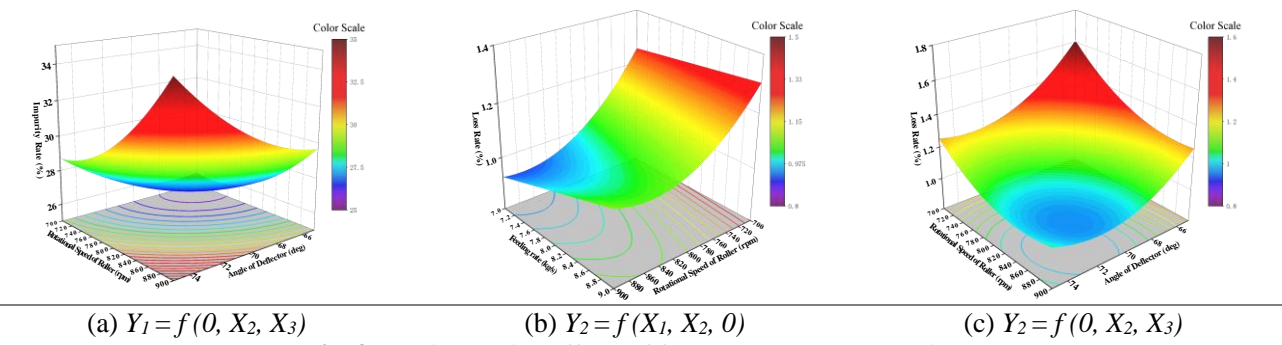


Fig. 8. The interaction effects of factors on threshed materials

Parameter Optimisation and Experimental Verification

With the optimisation objectives of minimising the impurity rate and loss rate, the parameter optimisation research on the wheat axial-flow threshing device was carried out. The constraint conditions for the objective function and factor variables were established as shown in Equation (4).

$$\begin{cases}
-1 \le X_i \le 1, i = 1, 2, 3 \\
0 \le Y_{j\min} \le 1, j = 1, 2 \\
\min Y_j, j = 1, 2
\end{cases}$$
(4)

Using Design Expert software to optimise and solve the multi-objective equations, the optimal parameter combination for wheat is obtained as follows: feeding rate 7 kg s⁻¹, drum

rotational speed 815 rpm, and guide plate angle 70 degrees.

To verify the accuracy of the prediction by each index model and the working quality of the optimised threshing device, further wheat threshing bench tests, field trials and discrete element simulations were conducted. The test results are presented in Table 9.

Table 9- Test results of optimised parameter combination

Item	Impurity rate (%)	Loss rate (%)
Predicted value of model	26.01	0.96
Value of validation test	25.02	0.95
Value of validation simulation	27.19	0.94
Relative error	3.81/4.54	1.04/2.08
Working quality of harvester	1.27	1.30

Discussion

Currently, there are relatively few discrete element simulations for the wheat threshing process. This is mainly because the method for constructing wheat plant models suitable for the threshing process lacks a theoretical basis, the bonding parameters of stems are difficult to determine, and the methods for verifying simulations are often not very convincing. These limitations have hindered the practical application of the discrete element method in the optimisation of threshing equipment, whereas this study has effectively addressed these issues through targeted methodological improvements.

In previous studies, significant progress has been made in the model construction and parameter calibration of wheat grains (Chen et al., 2020; Horabik et al., 2020; X. Wang et al., 2023). As noted in the studies by Sun et al. (2023) and Wang, Mao, and Li (2020b), neglecting minor components of wheat plants, such as awns and leaves, has little impact on the morphological, geometric, and mass parameters of wheat plant populations. Thus, in this study, the model construction of nonkey observation objects, including awns, glumes, and leaves, was neglected. Zhou et al. (2023) used the X-ray Tomography method to acquire the point cloud structure of wheat grains when constructing the wheat grain model, which is a more accurate model construction approach. However, wheat exhibits natural variations during its natural growth process. In this study, calibration of parameters such as the standard deviation of the normal distribution and bulk density was

introduced to reduce the uncertainty in model density caused by natural variations in the volume between real wheat grains and the model.

The construction of the wheat stem model is also critical for realising the threshing process simulation of wheat plants. Sun et al. (2023) constructed a wheat plant model with a high degree of fidelity, which is worthy of learning in terms of methodology, thinking, and logic. The difference lies in the treatment of spike model construction: Sun et al. added connecting spheres as the connecting medium between grains and the rachis. Wang, Mao, and Li (2020a) have realised the discrete element simulation of tangential threshing for rice. However, the modelling method is not applicable to axialflow threshing devices with a large feeding The sphero-cylindrical stem model adopted in this study addresses the issue of excessive particle count, reducing the number of particles per wheat plant from hundreds to 46. which significantly improves computational efficiency. Schramm Tekeste (2022) provided a theoretical basis for threshing simulation research through their work on parameter measurement calibration of wheat stems. But it did not further conduct research on the discrete element simulation of threshing. This study effectively verified the feasibility of threshing simulations by comparing the material distribution law at the bottom of the threshing obtained device from bench tests simulations. Miu and Kutzbach (2008a, 2008b) established a complete mathematical

model of the grain feeding, threshing, and separation processes, with the simulation results consistent with experimental data. However, this method merely involves statistics and analysis of threshing outcomes and cannot reconstruct threshing phenomena or reveal threshing mechanisms. Compared with studies focusing on statistical analysis of threshing results, our approach reconstructs the dynamic threshing process at the particle scale, enabling the revelation of mechanisms (e.g., force transmission between stems and grains, trajectory characteristics of detached grains) that are difficult to capture by purely statistical methods.

Building on the work of predecessors, this study completed such tasks as the construction of wheat models, the establishment of threshing benches, threshing simulations, and the exploration of threshing mechanisms. The implementation of these efforts can address existing issues in the current development of threshing technology. For instance, the performance test methods for traditional threshing devices are characterised by high cost, poor repeatability, long cycle, and high labour demand. Additionally, their internal threshing process is difficult to directly observe, making it impossible to further study the interaction between wheat and threshing components, among other problems.

However, this study also has several limitations. Based on the analysis and research presented in this paper, future research will focus on the following aspects: (1) There are significant differences in threshing performance under dry and wet threshing conditions. Moisture content will be taken as a variable to test its interaction with the current parameters. (2) Considering the impact of different wheat varieties on discrete element models (DEM), a wheat model with stronger generalisation ability will be established, and its adaptability will be verified. (3) DEM simulation has high computational requirements and is not suitable for real-time applications. In the future, we will further explore the potential of combining DEM with lightweight models in reducing the cost of real-time applications, as well as simplified modelling strategies for large-scale agricultural systems.

Conclusion

- (1) The discrete element parameters of wheat plants were measured and optimised using methods such as the inclined plane method, compression test, tensile test, and statistical principles. Additionally, rationality of the simulation was verified with the law of mass distribution of materials at the bottom as the evaluation index. The results show that the threshing simulation and the bench test are consistent in the law of mass distribution of materials at the bottom, indicating that the discrete element model of wheat plants constructed in this study is suitable for research on the wheat threshing process.
- (2) Using EDEM to analyse the movement patterns of wheat plants in the threshing device, the average velocity and force-bearing laws of wheat particles were obtained. It was found that stems, as carriers of grains, dominate the movement of grains during the feeding and impurity discharge processes. In the threshing and separating sections, there are significant differences in the movement patterns between grains and stems. Violent and unstable impact forces are the direct driving force for grain detachment. The maximum velocity of particles occurs in the impurity discharge section, reaching 7.3 m s⁻¹. The maximum force borne by particles occurs in the separating section, amounting to 184.8 N.
- (3) Through EDEM simulation and response surface optimisation experiments, the optimal parameters for the threshing device used in the experiment were determined as follows: a feeding rate of 7 kg s⁻¹, a drum rotation speed of 815 rpm, and a guide plate angle of 70 degrees. Bench verification experiments before and after optimisation showed that the wheat grain impurity rate decreased from 29.19% to 25.02%, and the loss rate decreased from 1.61% to 0.95%, with the error between the model prediction results

and the experimental results being less than 5%.

Funding: This research was funded by the National Key Research and Development Program of China, grant number 2022YFD2300803; Major Science and Technology Programs in Henan Province, grant number 221100110800; and Major Science and Technology Special Project of Henan Province (Longmen Laboratory First-class Project), grant number 231100220200.

Authors Contribution

- Q. Li: Conceptualization, Methodology, Data acquisition, Software services, Computer simulation, Visualization
- Y. Wu: Statistical analysis, Data pre and post processing, Text mining, Review and editing services

K. Zhao: Technical advice

H. Wang: Validation

J. Ji: Supervision

References

- 1. Ajmal, M., Roessler, T., Richter, C., & Katterfeld, A. (2020). Calibration of cohesive DEM parameters under rapid flow conditions and low consolidation stresses. *Powder Technology*, *374*, 22-32. https://doi.org/10.1016/j.powtec.2020.07.017
- 2. Arnold, P., & Roberts, A. (1969). Fundamental aspects of load-deformation behavior of wheat grains. *Transactions of the ASAE*, *12*(1), 104-0108. https://doi.org/10.13031/2013.38773
- 3. Boac, J. M., Ambrose, R. P. K., Casada, M. E., Maghirang, R. G., & Maier, D. E. (2014). Applications of Discrete Element Method in Modeling of Grain Postharvest Operations. *Food Engineering Reviews*, 6(4), 128-149. https://doi.org/10.1007/s12393-014-9090-y
- 4. Chen, Z., Wassgren, C., Veikle, E., & Ambrose, K. (2020). Determination of material and interaction properties of maize and wheat kernels for DEM simulation. *Biosystems Engineering*, 195, 208-226. https://doi.org/10.1016/j.biosystemseng.2020.05.007
- 5. Fu, J., Chen, Z., Han, L. J., & Ren, L. Q. (2018). Review of grain threshing theory and technology. *International Journal of Agricultural and Biological Engineering*, 11(3), 12-20. https://doi.org/10.25165/j.ijabe.20181103.3432
- 6. Horabik, J., & Molenda, M. (2016). Parameters and contact models for DEM simulations of agricultural granular materials: A review. *Biosystems Engineering*, 147, 206-225.
- 7. Horabik, J., Parafiniuk, P., & Molenda, M. (2016). Experiments and discrete element method simulations of distribution of static load of grain bedding at bottom of shallow model silo. *Biosystems Engineering*, 149, 60-71. https://doi.org/10.1016/j.biosystemseng.2016.06.012
- 8. Horabik, J., Wiacek, J., Parafiniuk, P., Banda, M., Kobylka, R., Stasiak, M., & Molenda, M. (2020). Calibration of discrete-element-method model parameters of bulk wheat for storage. *Biosystems Engineering*, 200, 298-314. https://doi.org/10.1016/j.biosystemseng.2020.10.010
- 9. Khawaja, A. N., & Khan, Z. M. (2022). DEM study on threshing performance of "compression-oscillation" thresher. *Computational Particle Mechanics*, *9*(6), 1233-1248. https://doi.org/10.1007/s40571-021-00456-4
- 10. Khir, R., Atungulu, G., & Pan, Z. (2013). *Influence of harvester and weather conditions on field loss and milling quality of rough rice*. Paper presented at the 2013 Kansas City, Missouri, July 21-July 24, 2013.
- 11. Lu, C., Gao, Z., Li, H., He, J., Wang, Q., Wei, X., ..., & Li, Y. (2023). An ellipsoid modelling method for discrete element simulation of wheat seeds. *Biosystems Engineering*, 226, 1-15. https://doi.org/10.1016/j.biosystemseng.2022.12.009
- 12. Luo, W., Chen, X., Guo, K., Qin, M., Wu, F., Gu, F., & Hu, Z. (2023). Optimization and Accuracy Analysis of a Soil-Planter Model during the Sowing Period of Wheat after a Rice Stubble Based Discrete Element Method. *Agriculture-Basel*, 13(10), 2036. https://doi.org/10.3390/agriculture13102036

- 13. Markauskas, D., Platzk, S., & Kruggel-Emden, H. (2022). Comparative numerical study of pneumatic conveying of flexible elongated particles through a pipe bend by DEM-CFD. *Powder Technology*, 399, 117170. https://doi.org/10.1016/j.powtec.2022.117170
- 14. Miu, P. I., & Kutzbach, H.-D. (2008a). Modeling and simulation of grain threshing and separation in axial threshing units: Part II. Application to tangential feeding. *Computers and Electronics in Agriculture*, 60(1), 105-109. https://doi.org/10.1016/j.compag.2007.07.004
- 15. Miu, P. I., & Kutzbach, H.-D. (2008b). Modeling and simulation of grain threshing and separation in threshing units—Part I. *Computers and Electronics in Agriculture*, 60(1), 96-104. https://doi.org/10.1016/j.compag.2007.07.003
- 16. Moya, M., Sanchez, D., & Ramon Villar-Garcia, J. (2022). Values for the Mechanical Properties of Wheat, Maize and Wood Pellets for Use in Silo Load Calculations Involving Numerical Methods. *Agronomy-Basel*, 12(6), 1261. https://doi.org/10.3390/agronomy12061261
- 17. Schramm, M., & Tekeste, M. Z. (2022). Wheat straw direct shear simulation using discrete element method of fibrous bonded model. *Biosystems Engineering*, 213, 1-12. https://doi.org/10.1016/j.biosystemseng.2021.10.010
- 18. Schramm, M., Tekeste, M. Z., Plouffe, C., & Harby, D. (2019). Estimating bond damping and bond Young's modulus for a flexible wheat straw discrete element method model. *Biosystems Engineering*, 186, 349-355. https://doi.org/10.1016/j.biosystemseng.2019.08.003
- 19. Shi, Y., Jiang, Y., Wang, X., Thuy, N. T. D., & Yu, H. (2023). A mechanical model of single wheat straw with failure characteristics based on discrete element method. *Biosystems Engineering*, 230, 1-15. https://doi.org/10.1016/j.biosystemseng.2023.03.017
- 20. Shi, Y., Sun, X., Wang, X., Hu, Z., Newman, D., & Ding, W. (2019). Numerical simulation and field tests of minimum-tillage planter with straw smashing and strip laying based on EDEM software. *Computers and Electronics in Agriculture*, 166, 105021. https://doi.org/10.1016/j.compag.2019.105021
- 21. Siliveru, K., & Ambrose, K. (2021). PREDICTING PARTICLE SEPARATION AND SIEVE BLINDING DURING WHEAT FLOUR SIFTING. *Transactions of the Asabe*, 64(3), 1103-1112. https://doi.org/10.13031/trans.14276
- 22. Standrads, A. (2006). Compression test of food materials of convex shape. In (Vol. S368.4). St. Joseph, Mich.: ASABE.
- 23. Sun, K., Yu, J., Zhao, J., Liang, L., Wang, Y., Yu, Y. J. C., & Agriculture, E. i. (2023). A DEM-based general modeling method and experimental verification for wheat plants in the mature period. *Computers and Electronics in Agriculture*, 214, 108283.
- 24. Wang, Q., Mao, H., & Li, Q. (2020a). Modelling and simulation of the grain threshing process based on the discrete element method. *Computers and Electronics in Agriculture*, 178, 105790. https://doi.org/10.1016/j.compag.2020.105790
- 25. Wang, Q., Mao, H., & Li, Q. (2020b). Simulation of Vibration Response of Flexible Crop Stem Based on Discrete Element Method. *Transactions of the Chinese Society of Agricultural Machinery*, 51(11), 131-137. https://doi.org/10.6041/j.issn.1000-1298.2020.11.014
- 26. Wang, W., Liu, W., Yuan, L., Qu, Z., He, X., & Lv, Y. (2020). Simulation and Experiment of Single Longitudinal Axial Material Movement and Establishment of Wheat Plants Model. *Transactions of the Chinese Society for Agricultural Machinery*, 51(S2), 170-180. https://doi.org/10.6041/j.issn.1000-1298.2020.S2.021
- 27. Wang, X., Wu, W., & Jia, H. (2023). Calibration of discrete element parameters for simulating wheat crushing. *Food Science & Nutrition*, 11(12), 7751-7764. https://doi.org/10.1002/fsn3.3693
- 28. Zareiforoush, H., Komarizadeh, M., & Alizadeh, M. (2010). Effects of crop-machine variables on paddy grain damage during handling with an inclined screw auger. *Biosystems Engineering*, 106(3), 234-242.

29. Zhou, Y., Shang, W., Hui, Y., Shi, C., Gao, J., Zhang, Y., ..., & Zhu, K. (2023). Construction of an Accurate Wheat-Grain Model Based on X-ray Tomography and Bonding Parameters by Discrete Element. *Applied Sciences-Basel*, *13*(16), 9265. https://doi.org/10.3390/app13169265

مدلسازی، شبیهسازی و آزمایش بهینهسازی: فرآیند خرمن کوبی گندم با کمباین بر اساس **DEM**

چیانون لی ۲۰۱^{*}، یوانزه وو^۱، کای شو آن ژائو^۱، های یوان وانگ^۲، جیانگ تائو جی ^{۲۰۱}

تاریخ دریافت: ۱۴۰۴/۰۴/۲۳ تاریخ پذیرش: ۱۴۰۴/۰۶/۱۱

جكيده

ریزش دانه و آسیب ناشی از ضربه، شاخصهای کلیدی کیفیت خرمن کوبی گندم هستند. برای بررسی مکانیسمهای ریزش و آسیب دانه، این مطالعه فرآیند خرمن کوبی گندم را با ایجاد یک مدل المان گسسته از گیاهان گندم و یک پلتفرم شبیهسازی برای دستگاههای خرمن کوبی بازتولید می کند. ایـن مطالعه شبیهسازی هایی را بر روی قوانین حرکت جریان مواد و قوانین توزیع مواد خرمن کوبی شده تحت شرایط مختلف نرخ تغذیه، سرعت چرخش درام و زاویه منحرفکننده انجام میدهد. بر اساس محاسبات شبیهسازی، قوانین سرعت و نیروی متوسط بوته های گندم بهدست اَمد و قوانین تاثیر نرخ تغذیه، سرعت چرخش درام و زاویه منحرف کننده بر فرآیند خرمن کوبی مورد تجزیه و تحلیل قرار گرفت. از طریق تجزیه و تحلیل بهینهسازی پارامتر چندهدفه، مشخص می شود که وقتی نرخ تغذیه ۷ کیلوگرم بر ثانیه، سرعت چرخش درام ۸۱۵ دور در دقیقه و زاویـه منحرفکننـده ۷۰ درجـه باشـد، خرمن کـوبی دستگاه عملکرد برتری دارد. آزمایشهای تایید آزمایشگاهی قبل و بعد از بهینهسازی نشان داد که میزان ناخالصی گندم از ۲۹/۱۹٪ به ۲۵/۰۲٪ و میزان تلفات از ۱/۶۱٪ به ۱۹۵٬ کاهش یافته است و خطای بین نتایج پیشبینی مدل و نتایج تجربی کمتر از ۵ درصد بوده است. مدل پیشنهادی و استراتژی بهینه سازی می توانند بهبود ساختاری دستگاههای خرمن کوب جریان محوری را هدایت کنند، چرخه تحقیق و توسعه تجهیزات برداشت را بهطور قابل توجهی کوتاه کنند و یک مبنای فنی قابل اعتماد برای برداشت کارآمد و کمضرر گندم فراهم کنند.

واژههای کلیدی: بهینه سازی پارامتر، تحلیل شبیه سازی، دستگاه خرمن کوب، روش المان گسسته، عملکرد کاری

۱ - دانشکده مهندسی تجهیزات کشاورزی، دانشگاه علوم و فناوری هنان، لویانگ ۴۷۱۰۰۳، چین ۲- مرکز نوآوری علمی و فناوری برای تجهیزات کامل، آزمایشگاه لونگمن، لویانگ ۴۷۱۰۲۳، چین

(*- نویسنده مسئول: Email: liqw0613@163.com)